Validation of Metal Volume Fraction Method and Mesoscale Finite Element Models; Predicting the Tensile Properties of GLARE

Lodewijk Bakker*, Daniel Calliess*, Adrian Ehrenberger*, Jacob Elskamp*, Ekaterina Konopleva*, Jonah Pedra*, Emma van Zutphen*and Lorenz Veithen*
Delft University of Technology, 2600 GB, Delft, The Netherlands

GLAss fibre REinforced aluminium laminate (GLARE) is a composite material made from metal sheets and glass fibre epoxy matrix layers. It belongs to a material class called Fibre Metal Laminates (FMLs). FMLs are commonly used in the aerospace industry due to their high strength to mass ratio. In order to assess the performance of different FMLs, numerical methods such as the Finite Element Method (FEM) or analytical schemes such as the Metal Volume Faction (MVF) are used. This study aims to identify the inaccuracies and describe the limitations of these predictive models for GLARE specimens under tensile load. To identify these inaccuracies, results from both the FEM and MVF methods were compared to each other and to experimental data from literature. Overall, the MVF method is less accurate at predicting the tensile properties of GLARE than FEM. While it is reasonably accurate for some GLARE types in the elastic region, it is inaccurate for the plastic region of all GLARE types. The FEM consistently overestimated the performance of the GLARE grades. However, it predicted the tensile properties to a high degree of accuracy. The MVF method is useful to obtain rapid and inexpensive results whilst sacrificing accuracy. FEM is used when higher accuracy is required, and more time can be dedicated to it. The likely sources of errors of FEM such as mesh size, boundary conditions and damage modes, need to be further investigated and are recommended focuses of research.

Keywords: fibre metal laminates, finite element method, metal volume fraction, tensile behaviour, GLARE

Nomenclature

E	=	E modulus, $[Pa]$
G	=	Fracture energy, $[K \cdot m^{-3}]$
P	=	Placeholder mechanical property
T	=	Traction force, $[N]$
t	=	Thickness, $[mm]$
u	=	Strain energy density, $[J/m^3]$
U_e	=	Elastic strain energy, $[J]$
δ	=	Separation length, $[mm]$
ϵ	=	Strain, [%]
μ_θ	=	Krenchel orientation factor, [-]
σ	=	Stress, $[Pa]$
VF	=	Volume fraction

Subscripts

c	=	Damage initiation (or critical)
co	=	Composite
f	=	Final
I	=	Tensile mode
II	=	Shear mode
metal	=	Metal layer
u	=	Ultimate
y	=	Yield
fib	=	fibre
e	=	epoxy

Superscripts

cr	=	Critical

Abbreviations

CZM	=	Cohesive Zone Model
FE	=	Finite Element
FEM	=	Finite Element Method
FML	=	Fibre Metal Laminate
GLARE	=	Glass Reinforced Aluminium Laminate
MVF	=	Metal Volume Fraction
TSL	=	Traction Separation Law

*Student Aerospace Engineering Faculty at TU Delft

I. Introduction

Fibre Metal Laminates (FMLs) are composite materials made from the combination of thin sheets of metal with fibre epoxy layers. The material is proving to be useful in many engineering solutions, as many of its properties can be manipulated by varying characteristics of the material, such as the fibre orientation, the material used and the structure of the layers [1]. Within the aerospace industry, FMLs are an ideal material for diverse applications, such as fuselage panels, due to their excellent fatigue strength and impact resistance [2].

Implementing FMLs in real aircrafts, however, involves careful testing and simulation and has only rarely been done on a large scale [3]. Developed at the Delft University of Technology, GLAss fibre REinforced aluminium laminates (GLARE) are promising FMLs that have successfully been used in the fuselage of the A380 aircraft. Simulations of FMLs are key to predict their behaviour under loading, locate potential problems and optimize a design. Accurate simulations of FMLs can help in creating more cost-effective and time-saving design processes. This is because accurate simulations require fewer specimens to be built and tested in order to validate a design.

Metal Volume Fraction (MVF) method is usually the first method that is used in order to estimate an FML's properties. The method takes into account the proportion of the different materials present in the FML to estimate the final tensile properties of the composite. It consists of a combination of the individual tensile properties of each material weighted by their quantity percentage [4], which usually is sufficient as a first-order approximation.

Finite Element Methods (FEM) are often used when more precise results are needed. Such a simulation is created in softwares like Abaqus. For FMLs, the level at which the simulation is evaluated usually occurs at the mesoscopic level. FEM on the mesoscopic level focuses on the behaviour of individual supplies and the interaction between each other [5]. The mesoscale level, therefore, allows analysing of both inter and intra-laminar damages occurring in FMLs. Damages such as delamination of the layers [6]. Both the alternative microscale and macroscale levels are unable to simulate damage events and the interaction between the layers [7].

A method that is used to create this simulation of the interaction at the mesoscale level, is the bilinear cohesive zone modelling method [5]. This method assumes that an adhesive between the plies is completely elastic until a critical traction force is reached. The process then continues plastically until no more resistance is provided by the cohesive zone [5], at this point in the FEM simulation, the adhesive can be said to have been fully delaminated.

Nevertheless, literature lacks acknowledgement of the accuracy of either model. These modelling methods are limited by their underlying assumptions and therefore do not account for an accurate reality of the FML behaviour. Furthermore, this lack of acknowledgement also limits the choice in preference between different methods, in this case being MVF and FEM.

This paper aims to identify the accuracy of the MVF and FEM methods for GLARE specimens under tensile load using experimental data. In the MVF method, the tensile properties of an FML are simply calculated and compared to the values of the experimental data. The process of the FEM method is a bit more extensive. At first a model is established in Abaqus, at the mesoscale level, with cohesive zone modelling. In this model, a range of different GLARE types is then simulated. Once this has been done, stress-strain curves can then be generated. These curves are then compared to experimental data, while specifically looking at the tensile properties: yield strength, ultimate tensile strength and E-modulus. The difference between these tensile properties reveals the error of the FEM in an attempt to reflect reality.

II. Materials and Methods

Table 1. GLARE Fibre Orientation Naming [8]

GLARE Grade	Fibre Orientations [deg]
2A	0/0
3	0/90
4A	0/90/0
5	0/90/90/0
6A	+45/-45

A total of 27 GLARE FML types were analysed, each could be classified by fibre orientation as one of the four different grades presented in Table 1 and by metallic ply thicknesses which can take values of 0.3, 0.4 and 0.5 mm. The make up of a single GLARE type can be inferred from its name. An example of such a name from one of the analysed GLARE types is GLARE 3 6/5-0.4. The 3 identifies the grade of the GLARE type, which in turn identifies the orientation of the fibres. 6/5 establishes that this specimen has 6 aluminium layers and 5 glass fibre layers. The number of aluminium layers is always one higher than that of the amount of glass fibre layers so that the glass fibre layers can always be sandwiched between 2 metal layers. The last part of the name, 0.4, describes the thickness of the aluminium in [mm].

The five different GLARE grades that were used

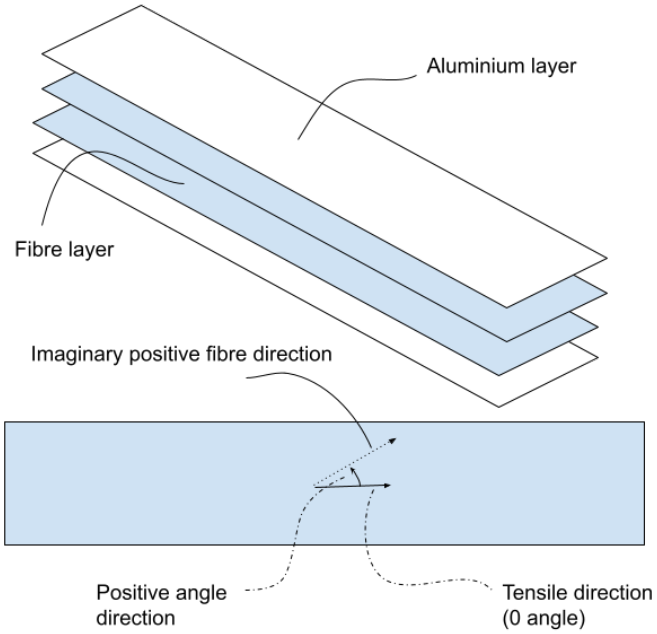

Figure 1. Fibre Angle Orientation [own work]

can be seen in Table 1 . The number of angles represents the number of fibre layers in the glass fibre layer. The angles are defined as the amount of anti-clockwise rotation from the direction in which the specimen experiences a tensile test. This direction is also referred to as the tensile direction. Figure 1 details this explanation.

The three aluminium thicknesses that were used were 0.3, 0.4 and 0.5 mm. These thicknesses were varied in different stacking sequences, but were consistent for each lay-up. Together with the variation in fibre direction, this thickness variation creates the total of 27 different Glare types seen in Table 3 from Appendix A.

The material properties for each of these 27 laminates were determined using three approaches: Metal Volume Fraction, Finite Element and experimental method. For each, the E-modulus, yield strength and ultimate strength of the material in the axial direction were determined with respective methods.

A. Database

The experimental data for the 27 considered GLARE types were gathered from [5, 9, 10]. The characteristics gathered, again consist of the same three parameters mentioned earlier, namely yield strength, ultimate strength and E-modulus. This data can be found in Tables 3 and 4 from Appendix A.

The experimental data of the 27 GLARE types were created with tensile tests that were in accordance with the ASTM D-3039 standard [5, 9–11]. This means that the dimensions of all the test specimens were very similar. In Figure 2 an example of these dimensions can be viewed.

Information on the behaviour of Aluminium and Glass/epoxy was also gathered as they are the main constituents of the FMLs considered [5, 12]. This included the E-modulus in the axial direction, yield and ultimate strength, and failure strain per component as shown in Table 5 from Appendix A. This data was used to determine the behaviours of the 27 laminates using the FEM and MVF methods as explained below. The results of the methods used are presented in Table 3 from Appendix A.

Similarly, the information needed for the FEM model in regards to the damage of the adhesive used for the bonding of the layers was taken from [13]. This includes damage initiation stresses (σ_{Ic} & σ_{IIc}), E-modulus (E), and fracture energies (G_{Ic} & G_{IIc}). The adhesive constants are shown in: Table 6 from Appendix A.

B. Data Acquisition

Within this section, the different data acquisition methods are outlined. This includes the data simulated in Abaqus, experimental and metal volume fraction data.

1. Simulation Data

As stated in subsection A, the experimental results of the GLARE types came from a tensile test in accordance with the ASTM 3039 standard [11]. Most authors [5, 9, 10] used specimens similar to this con-

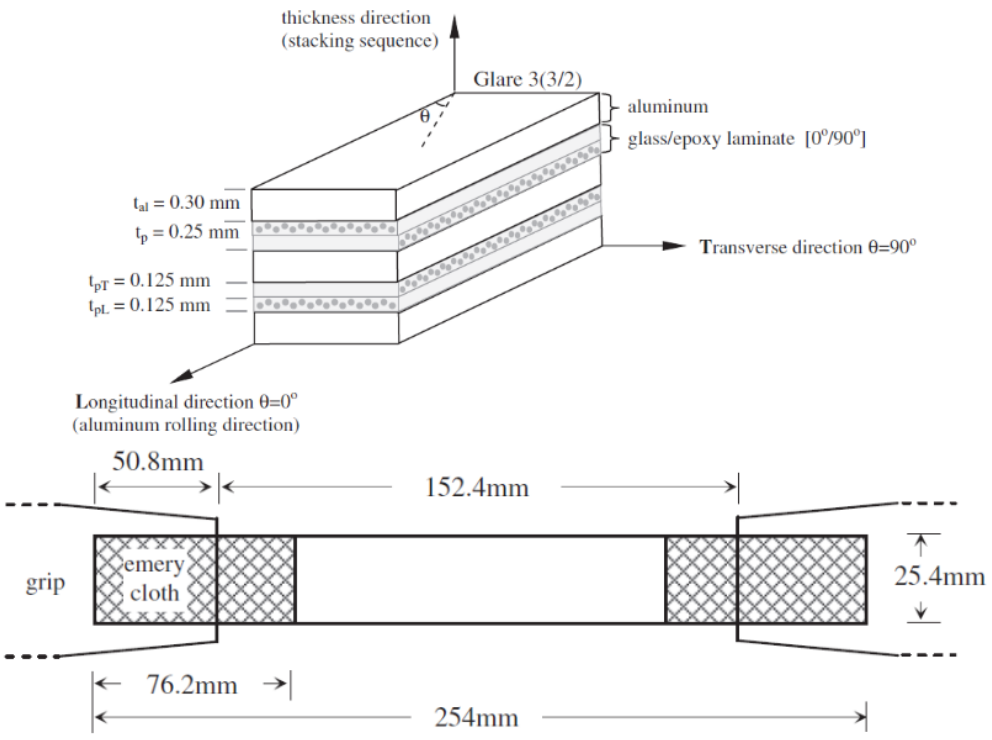

Figure 2. Typical specimen used in Finite Element Method [9, p.111]

vention for their experimental work. Therefore, the dimensions of the specimens from [9] were used to simulate a tensile test in the FEM software, to accurately compare the data of the simulation to the experiments. The dimensions of this specimen can be seen in Figure 2.

In creating an FML in FEM software, two main methods can be used to simulate the interaction between layers of a composite layup: a friction coefficient or Cohesive Zone Modelling (CZM). The difference between the two being that CZM also simulates the failure due to delamination, which is the process where the shear forces exceed the maximum shear of the adhesive causing separation of the layers. A constant friction coefficient fails to account for adhesive failure therefore CZM was used in the FEM model. Consequently, the GLARE FMLs were all abstracted to three distinct components for Abaqus: a glass epoxy component, an aluminium component and an adhesive component.

The aluminium component was modelled using a C3D8R element, a general-purpose linear brick element with eight nodes. It is commonly used for isotropic materials and metals [14].

For the glass epoxy component, however, ductile behaviour is not the main failure mode. The damage that leads to failure of the glass epoxy component was instead modelled using the Hashin damage criterion, a damage progression model for modelling non-metal plies in FMLs [15]. For this damage criterion, only a continuum shell model with eight nodes can be used (element SC8R).

The COH3D8 element was used for the adhesive layer. This is an element that can model the primary forces that are large within the adhesive, namely shear. Damage due to shear must be modelled using a traction separation law. In order to create a bilinear cohesive zone, a maximum damage law was selected in Abaqus. Based on the method by Al-Azzawi et al. a thickness of 0.01 mm was used for the adhesive layer [13]. The COH3D8 element also enables the correct type of bonding between layers. The cohesive layers are placed between each layer which was connected with a Tie constraint, restricting any movement between the two.

The boundary conditions that model the force applied to this specimen are set for each lay-up. In each, two boundary conditions are set and are applied over the normal surface area at each end of the specimen. This is to simulate every layer being pulled outward by the grip in the experimental test A. The tensile force created by this boundary condition was then used to calculate the E-modulus, the yield strength and the ultimate strength.

The history output was configured such that it gave the displacement of the boundary at the free end of the specimen at a certain time, as well as the total amount of force generated by the boundary con-

dition in order to pull the lay-up out as far as that displacement. The stress and strain were then calculated using specimen cross-sectional area and length.

2. Experimental Data

The experimental data used in this study was gathered from literature [9, 10]. Although different authors used various testing procedures, the results' accuracy does not vary significantly from one to another. The authors recommend [11] for specifications on the test setup.

3. Metal Volume Fraction

To analyse relative accuracy of FEM, a theoretical approach was considered. The Metal Volume Fraction is the simplest theoretical method known to literature that is capable of predicting the laminate properties [16].

The composite present in the FML is assumed to be orthotropic, meaning it behaves differently in the three perpendicular directions. Furthermore, the relationship between stress and strain is assumed to be bilinear until the point of failure for simplicity. In order to describe the linear response, two elastic moduli E_1 and E_2 are used, measured in the direction of the fibres and the perpendicular to that direction.

The metal layer behaviour can be described using Hooke's law for the linear elastic region. A model from [17] is used to explain the plastic behaviour after the yield stress has been surpassed.

MVF is the ratio between the total thickness of the metal sheets and the total thickness of the FML, as given by the following equation [16]:

$$MVF = \frac{\sum t_{metal}}{t_{FML}}. \tag{1}$$

Any material property P_{FML} of the considered FML is then given by: [16]

$$P_{FML} = MVF \cdot P_{metal} + (1 - MVF) \cdot P_{composite} \tag{2}$$

4. Krenchel's Factor for Fibre Orientation

Material property data for the epoxy-glass layers found from the literature ([12]) was only given in 0° and 90° direction. To calculate the material properties of GLARE 6A, having 45° fibre orientations the simple MVF method is not sufficiently accurate. This is the case for all Glare 6A 2/1 composites, where the cross plies are orientated at a 45 deg angle relative to the loading direction. Therefore, the modified MVF method is used, which utilises Krenchel's factor to account for the arbitrary loading angle [18];

$$E_{co} = \eta_\theta \cdot E_{fib} \cdot VF_{fib} + E_e \cdot VF_e \tag{3}$$

where, E_{co} is the E modulus of the composite layers in the FML. E_{ib} and VF_{fib} stand for the E modulus and volume fraction of the fibres. E_e and VF_e stand for the the E modulus and volume fraction of the epoxy matrix. In accordance with [18] for a cross-ply orientation of 45 degrees;

$$\eta_\theta = cos(\theta)^4 = 0.25 \tag{4}$$

The E modulus obtained form Equation 3 can then be used in Equation 2 in order to calculate the mechanical property of the complete FML.

C. Data Processing and Representation

This section explains how the data, acquired through the methods discussed in subsection B, is processed into graphs for further analysis using Python and Excel. These graphs include stress-strain graphs and bar charts showing different tensile properties.

1. Stress-strain Curves

Stress-strain curves of GLARE laminates were generated from the results of the aforementioned methods under the assumption of bilinear behaviour well known for FMLs [5].

Given information about the E-modulus, yield strength and ultimate strength, three data points can be deduced under the following two assumptions: the strain at zero stress is zero (the graph goes through the origin) and the strain at ultimate stress is the strain of the composite layers at failure as the metal would not be able to support the complete load after composite failure. This gives a set of three points: (0, layer0); (ϵ_y, σ_y); (ϵ_u, σ_u).

The curves were then plotted through these three points using linear splines according to the bilinear behaviour mentioned earlier. Once the graphs of each FML using different methods are obtained, comparisons are performed by plotting different curves in the same graphs. In this way, graphs for comparison of the stress-strain curves obtained from MVF, FEM and experimental methods can be obtained.

2. Bar Charts

Bar charts were used to represent and compare specific parameters obtained using different methods. The parameters in question are tensile properties: E-modulus, yield strength and ultimate strength.

III. Results and Discussion

To verify the accuracy of the results obtained from the FEM and MVF methods described in section II, the results are compared with the experimental data.

In this section, the most relevant graphs for analysis are outlined in subsection subsection A and results are stated for further discussion in subsection B.

A. Results

Figure 3 shows the stress-strain curve obtained for GLARE 2A 2/1-0.5 comparing the two methods (FEM and MVF) and the experimental results. FEM systematically overestimated yield stress and E-modulus for all GLARE types analysed.

When analysing the graphs, an anomaly was found in the data in regards to GLARE 6A 2/1-0.5 (Figure 4). The mechanical properties for this GLARE lay-up were strikingly overestimated by FEM, with differences of up to 26.8% present when comparing the FEM to the experimental data (Figure 6). For GLARE 6A 2/1-0.4, the same lay-up with 0.1 mm thinner metal sheets, FEM matched the experimental results with a high degree of accuracy. A change in thickness of only 0.1 mm should not cause FEM to suddenly become inaccurate and therefore the result for GLARE 6A was discarded and attributed to an incorrect FEM setup.

The MVF method shows larger disagreement from experimental results than FEM as seen in Figures 3 to 6. Both E-modulus and ultimate stress values are either over or underestimated depending on the layup and GLARE type, but no specific pattern was observed, contrary to FEM results. The E-modulus was observed to be overestimated for GLARE 2 and 4 and underestimated for GLARE 3, 5 and 6.

It was observed that the yield stress results from the MVF method are underestimated for low MVF numbers and overestimated for high MVF numbers. These are also presented on top of the stress-strain graphs presented.

In Figure 7 the ultimate stress values for different GLARE types are shown which cannot be seen in the stress-strain graphs. It is evident that FEM overestimates the ultimate strength across all GLARE grades. The MVF method again fluctuates depending on the material.

A numerically comparative method that is used for the evaluation of the two predictive methods is the Mean Squared Error (MSE), described in Table 2. The MSE was calculated for all GLARE specimen excluding anomalous readings. This demonstrates that the MVF method has considerably larger errors in yield stress, ultimate stress and E-modulus results in comparison to FEM.

Table 2. MSE for different methods with respect to experimental results [own work]

	E [GPa]	σ_{yield}[MPa]	σ_{ult} [MPa]
MVF	4.85	110.62	992.29
FEM	0.96	17.66	50.53

B. Discussion and Explanation of Results

1. *MVF Divergence*

From the data, certain patterns that MVF estimates adhere to can be observed. Most prominently, the MVF approximations for the 6A GLARE type are much less accurate than for other GLARE types as they include $[45°, -45°]$ layers, the behaviour of which is hard to predict theoretically. Furthermore, it has been observed that the MVF method consistently overestimates the properties for $[0°, 0°]$ grades and mostly underestimates them for the $[0°, 90°]$ grades. No similar pattern is observed in other GLARE lay-ups.

The MVF method presented earlier is derived from Hooke's Law, limiting the use of MVF as an effective predictor to the linear elastic region. This is seen in Table 2 with the MVF results having considerably more error for the ultimate stress prediction, happening in the plastic region, than the elastic region properties.

The discrepancies between the MVF estimations and data obtained experimentally are likely caused by various factors that impact the stress/strain curve in modest but noticeable ways. Examples of these factors include: inter-layer interaction, inter-fibre interaction, material defects from manufacturing, assuming no micro-structure is present and instead considering the complete glass-epoxy layers to be homogeneous, amongst others. Approximating the glass-epoxy layer as a homogeneous material leads to the material property values for this layer to be inaccurate because micro-scale damage, such as crack propagation, and fibre-matrix interaction are ignored. This is the case for both fibre directions and depending on the GLARE type and layup analysed. This resulted in sometimes overestimated and underestimated properties. In particular, the [0, 0] lay-up which is overestimated and the [0, 90] lay-up which in contrast is underestimated.

2. *FEM Divergence*

As described in subsection A, FEM tends to consistently overestimate the results of the specimens compared to the experimental data. The cause of which is therefore unlikely to be instability of the test and rather a systematic error. The most likely of which are discussed here.

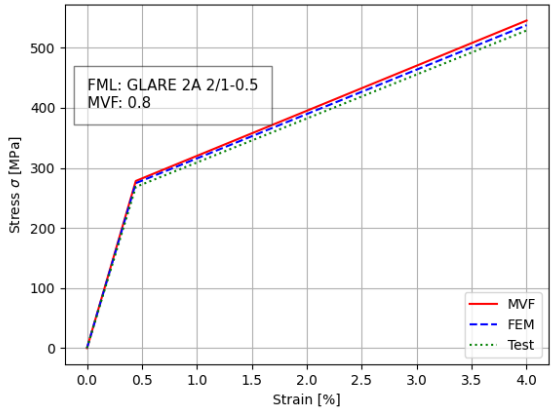

Figure 3. stress-strain curve of Glare 2A 2/1-0.5 obtained from the two predictive methods and the experimental data [own work]

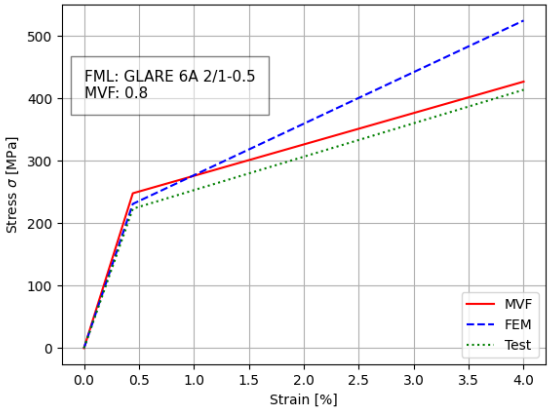

Figure 4. stress-strain curve of Glare 6A 2/1-0.5 obtained from the two predictive methods and the experimental data [own work]

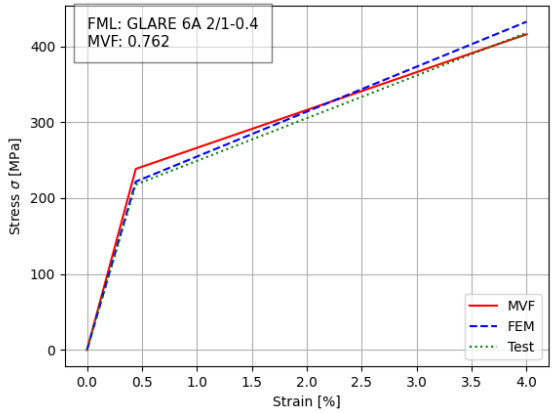

Figure 5. stress-strain curve of Glare 6A 2/1-0.4 obtained from the two predictive methods and the experimental data [own work]

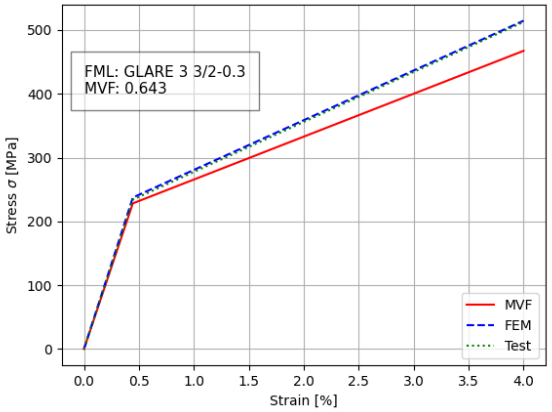

Figure 6. stress-strain curves of GLARE 3 3/2-0.3 obtained from the two predictive methods and the experimental data [own work]

Firstly, the error may be in regards to the constituent materials. Within the simulation, a mesoscale level abstraction was used which makes the program unable to factor in impurities on the microscale such as those introduced by manufacturing errors. Nevertheless, it is expected that the constituent material experimental data includes such impurities. Errors like improperly applied adhesive, however, resulting in thinner and thicker regions of adhesive in the lay-up, are not accounted for in this reducing the maximum stress that an experimental specimen can withstand.

Furthermore, the mesh size is another expected factor in the overestimation of the results. This has to do with discretizing the material into a mesh with different volume elements. These volume elements are the smallest elements in which stress concentrations are calculated within the simulation. Consequently, the error may be sourced from generalising the stress concentrations instead of focusing on specific points. This, in turn, creates lower stress concentrations. For example, a starting crack as a result of improper manufacturing may have a significantly higher stress concentration. In such a case, the simulation would overestimate the capability of the specimen to carry load compared to the experimental data.

As described in the Simulation Data section (subsubsection 1) of Methods, there are three damage modes used in the model: Hashin damage, ductile damage and the Traction Separation Law (TSL). Two of these damage models use an idealisation that makes it possible to explain the tensile property results divergence of the FEM model compared to the experimental results. Damage according to the

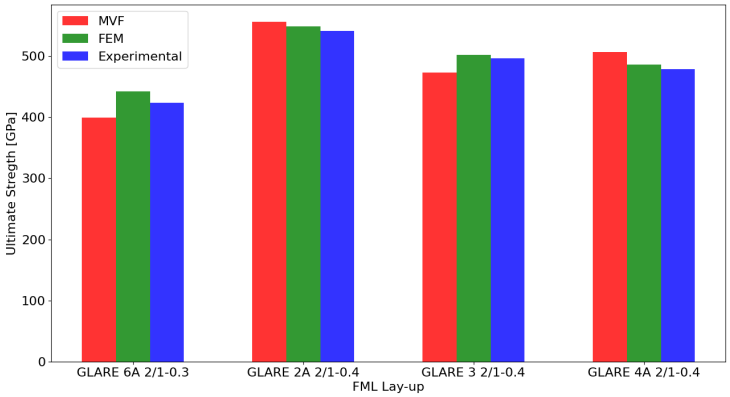

Figure 7. Ultimate strength of different GLARE types obtained from the two predictive methods and the experimental data [own work]

Hashin damage method, for example, does not include crack propagation in its prediction [19]. Crack propagation will cause earlier failure due to the lack of material to withstand the increased stress and strain. The TSL in turn, leads to behaviour such that there is a "significant artificial elastic range that is not controllable" [20, p.17]. This shows that the E-modulus particularly could be inaccurately determined by this damage mode.

The final damage mode, ductile damage, should not cause much modification of the results. The reason for this is that the ductile damage mode is initiated when the aluminium material's ultimate stress is passed. The ductile damage mode can then model the behaviour after this ultimate stress. However, aluminium has little or no energy during fracture, as demonstrated in Figure 8 where aluminium shows no data after the ultimate stress in comparison to steel. This means that there is almost no necking and practically immediate failure for when the ductile damage mode is initiated.

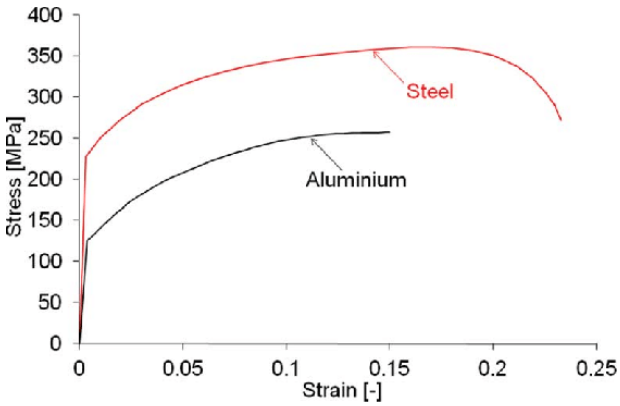

Figure 8. Stress-strain curve of aluminium vs. steel [21, p.169]

In FEM, the boundary conditions are applied on every constituent of the FML and therefore there is no difference in force applied between the different layers. In reality, the specimen is clamped only on the outer plies of the FML, resulting in a shear force pulling the inner plies out instead of an axial force acting in the same manner. One can deduce that having the boundary conditions applied to every layer of the FML results in higher maximum stress values. In the model used, no added shear-induced in-between layers as a result of a force only pulling the outer plies. This overestimates the force at which the adhesive in the specimen would fail and therefore the idealisation of the boundary conditions could be the cause of very significant discrepancies between the experimental results and FEM results.

3. Validity

Data obtained from experimental tests were used to determine the accuracy of the results obtained from Abaqus simulations and the MVF method. The experimental data is limited to what has been published by other authors; no experimental work has been carried out in the framework of this research. For validation, the work presented by [22] was used as it presents multiple experimental datasets.

The exact instrumentation to obtain the experimental results is unknown. Furthermore, it is also unknown if the instrumentation used varies across the data collected. This makes it difficult to judge the validity of the experimental results. Ergo, the study may contain uncertainties and errors, however on a scale that is not significant for this research and does not affect the judgement of the results.

4. Comparison to Published Work

Historic experimental data was obtained for comparison to obtained experimental values [9], using B-

Splines to then interpolate the data. Ergun et al. [9] used a similar approach for the MVF predictions of FMLs and came to the same conclusion that the GLARE 3 3/2-0.3 stress-strain curve is underestimated by the method, as was found in this work. For the cross-ply properties, [9, p. 118] uses a different method considering empirical data. In this work, a more general composite approach named the Krenchel's factor for Fibre Orientation was used [18]. The latter was found to be more straightforward to use and to yield satisfying results.

FEM analysis matched the experimental results very closely for all GLARE types that were investigated. FEM has a much lower MSE compared to the MVF method, see Table 2. This observation is supported by previously published articles [5]. However, it is very important to set up the model properly and choose an appropriate scale to run the analysis, this is described in some detail in subsection B as well as in [5, 13]. FEM results used in this article were obtained from analysing an FML at the mesoscale. This is supported by a study comparing the three main FEM scales [23].

IV. Conclusion

The tensile performance of five GLARE grades is predicted using the Metal Volume Fraction method and a Finite Element simulation. This data is compared to experimental results and the found discrepancies are discussed.

The MVF method has a significantly lower accuracy overall compared to FEM. The MVF method commonly used for cross-ply grades was deemed too inaccurate to be used. Therefore, the GLARE 6A grades ($[+45°/-45°]$) properties were estimated using an MVF method with the Krenchel's factor [18]. Still, MVF predicted 6A properties the worst. It was also noted that MVF predicts E-modulus far better than yield or ultimate strength. The accuracy of MVF, although worse, can be comparable to the FEM method for the E-modulus. Ergo, MVF can prove to be useful in the early design stages when quick availability of the results is prioritized over accuracy.

It was found that the FEM results consistently overestimated the performance of GLARE types, such as GLARE 6A 2/1-0.5 with an overestimation of mechanical properties up to 26.8%. A possible cause for this is uncertainty in the boundary conditions, along with discretization errors. In addition, imperfections in the manufacturing process of the GLARE layups are difficult to model in a FEM simulation contributing to the overestimation. This is in part due to limitations of the software used by the authors to obtain the FEM data.

The graphs presented in this research were solely based on three parameters along with the assumed ultimate strain, namely: the E-modulus, the yield stress and the ultimate stress. This limits the accuracy of the results derived from these graphs as it required the assumption of bi-linear behaviour well-known to most FMLs. A difference in this behaviour would not have been observed in this study.

Overall, the aim was to identify the inaccuracies within these models and as described above these were identified yet, difficult to explain. The source of such errors is hard to locate due to the lack of parameters and detail involved in these methods, for example, this report only focuses on one scale (mesoscale).

Further research is required to assess in more detail the reasons behind the overestimation of the tensile behaviour by FEM with respect to the experimental results obtained. This may include, doing research into the alternative two scales in FEM; micro and macro and comparing results to discover the source of error. Or, more parameters could be compared other than the three existing tensile properties to identify more aspects of the method that could involve inaccuracies, for example, the offset yield strength.

Acknowledgments

This research was carried in the context of a second-year BSc project at the faculty of Aerospace Engineering at the Delft University of Technology. The authors want to thank Shichen Liu for his assistance by sharing his expertise throughout the research and Angeniet Kam for providing help to follow the scientific writing conventions.

References

[1] Z. Ding, H. Wang, J. Luo, and N. Li. "A review of forming technologies of fibre metal laminates". *International journal of lightweight Materials and Manufacture.* vol. 4, n. 1,p. 110-126, 2021, Available: ScienceDirect `https://doi.org/10.1016/j.ijlmm.2020.06.006`.

[2] T. Sinmazçelik, E. Avcu, M. Özgür Bora, and O. Çoban. "A review: Fibre metal laminates, background, bonding types and applied test methods". *Materials & Design.* vol. 32, n. 7, p. 3671-3685, 2011, Available: Elsevier, `https://doi.org/10.1016/j.matdes.2011.03.011`.

[3] J. Sinke. "Development of fibre metal laminates: Concurrent multi-scale modeling and testing". *Journal of Materials Science*. vol: 41, n. 20, p. 6777-6788, 2006, Available: Springer. https://doi.org/doi:10.1007/s10853-006-0206-5.

[4] R. Alderliesten. *Fatigue and Fracture of Fibre Metal Laminates*. Springer International Publishing AG, 2017. https://doi.org/10.1007/978-3-319-56227-8.

[5] P. Soltani, M. Keikhosravy, R.H. Oskouei, and C. Soutis. "Studying the tensile behaviour of glare laminates: a finite element modelling approach". *Applied Composite Materials*. vol. 18, n. 4, p. 271-282, 2011, Available: Springer, https://doi.org/10.1007/s10443-010-9155-x.

[6] R. Karthikayen, T. Tay, and V. Tan. "A review of the FE^2 method for composites". *Multiscale and Multidisciplinary Modeling, Experiments and Design*. vol. 4, p. 1-24, 2021, Available: Springer, https://doi.org/10.1007/s41939-020-00087-x.

[7] A. Forghani, M. Shahbazi, N. Zobeiry, A. Poursartip, and R. Vaziri. "An overview of continuum damage models used to simulate intralaminar failure mechanisms in advanced composite materials". *Woodhead Publishing Series in Composites Science and Engineering*. p. 151-173, 2015, Available: ScienceDirect, https://doi.org/10.1016/B978-0-08-100332-9.00006-2.

[8] FMLC. Results & cases, n.d. Fibre Metal Laminate Centre of Competence.

[9] H. Ergun, B.M. Liaw, and F. Delale. "Experimental-theoretical predictions of stress–strain curves of glare fiber metal laminates". *Journal of Composite Materials*. vol. 52, p. 109, 2017, Available: SAGE journals. https://doi.org/10.1177/0021998317702954.

[10] A. Vlot and J.W. Gunnink. *Fibre Metal Laminates : an Introduction*. Springer Science+Business Media, 2001. https://doi.org/10.1007/978-94-010-0995-9.

[11] ASTM International. *Standard Test Method for Tensile Properties of Polymer Matrix Composite Materials*. ASTM International, 2002. https://doi.org/10.1520/D3039_D3039M-17.

[12] MatWeb. Matweb - material property data, 2021. http://www.matweb.com/.

[13] A.S.M. Al-Azzawi, L.F. Kawashita, and C.A. Featherston. "A modified cohesive zone model for fatigue delamination in adhesive joints: Numerical and experimental investigations". *Composite Structures*. vol: 225, 2019, Available: Elsevier. https://doi.org/10.1016/j.compstruct.2019.111114.

[14] Dassault Systèmes. 28.1.4 three-dimensional solid element library, 2014. Abaqus Analysis User's Guide.

[15] A.P.C. Duarte, A. Díaz Sáez, and N. Silvestre. "Comparative study between xfem and hashin damage criterion applied to failure of composites". *Thin-Walled Structures*. vol. 115, p. 277-288, 2017, Available: Elsvier, https://doi.org/10.1016/j.tws.2017.02.020.

[16] S. van der Zwaag. AE1108. Class Lecture, Topic: "Stiffness polymers composites and selection" Faculty of Aerospace Engineering, Delft Technical University, Delft, NL, 2019.

[17] V.P. Bouwman. A calculation tool for structural analysis of general laminates, 2002. report number: nlr-cr-2002-44.

[18] Peter Hine, Bushra Parveen, and Dave Brandsand Fin Caton-Rose. "Validation of the modified rule of mixtures using a combination of fibre orientation and fibre length measurements". *Composites Part A: Applied Science and Manufacturing*. vol. 64, p. 70-78, 2014, Available: Elsevier, https://doi.org/10.1016/j.compositesa.2014.04.017.

[19] Álvaro Díaz Sáez. "Finite element modelling of damage and failure in fiber reinforced composites". *Composites Part A: Applied Science and Manufacturing*, 2016.

[20] P.Kyoungsoo and G.H.Paulino. "Cohesive zone models: A critical review of traction-separation relationships across fracture surfaces". *Applied Mechanics Reviews*. vol. 64, 2011, Available: ASME, https://doi.org/10.1115/1.4023110.

[21] Bin Liu, Richard Villavicencio, and Carlos Guedes Soares. Failure characteristics of strength-equivalent aluminium and steel plates in impact conditions. 2013. 10.1201/b15120-25.

[22] G. Wu and J. Yang". "Analytical modelling and numerical simulation of the nonlinear deformation of hybrid fibre–metal laminates. *Modelling and Simulation in Materials Science and Engineering.* vol. 13, p. 413-425, 2005, Available: Institute of Physics Publishing, http://dx.doi.org/10.1088/0965-0393/13/3/010.

[23] M. Smolnicki and P. Stabla. "Finite element method analysis of fibre-metal laminates considering different approaches to material model". *SN Appl. Sci.* vol. 1, p. 467, 2019, Available: Springer, https://doi.org/10.1007/s42452-019-0496-2.

A. Database of Fibre Metal Laminates

This appendix presents some figures to support explanations used in the rest of the paper.

Table 3. Data acquired for this work

FML type	t (mm)	FEM result			Experimental test result		
		E (GPa)	σ_y (MPa)	σ_{ul} (MPa)	E (GPa)	σ_y (MPa)	σ_{ul} (MPa)
GLARE 2A 2/1-0.3	0.85	67.4	256.4	567.5	66.2	248.3	558.2
GLARE 3 2/1-0.3	0.85	63.5	242.6	510.2	62.7	237.5	503.6
GLARE 4A 2/1-0.3	0.98	61.4	235.7	495.3	60.8	232.1	489.7
GLARE 5 2/1-0.3	1.10	60.8	219.4	469.6	58.2	216.5	462.8
GLARE 6A 2/1-0.3	0.85	62.3	208.2	442.1	61.5	205.1	423.6
GLARE 2A 2/1-0.4	1.05	68.0	265.4	548.9	67.3	259.6	541.5
GLARE 3 2/1-0.4	1.05	65.7	254.8	502.6	64.6	249.5	496.7
GLARE 4A 2/1-0.4	1.18	63.8	248.6	486.4	62.3	243.7	478.9
GLARE 5 2/1-0.4	1.30	61.5	226.2	466.9	60.7	223.8	458.1
GLARE 6A 2/1-0.4	1.05	64.2	215.4	432.4	63.4	211.7	417.8
GLARE 2A 2/1-0.5	1.25	69.4	270.6	537.5	68.3	264.1	528.7
GLARE 3 2/1-0.5	1.25	66.8	256.8	494.3	65.5	252.9	487.8
GLARE 4A 2/1-0.5	1.38	64.3	249.6	473.2	63.2	246.5	465.1
GLARE 5 2/1-0.5	1.50	63.2	231.4	452.1	62.4	228.7	446.5
GLARE 6A 2/1-0.5	1.25	65.4	222.3	524.5	64.7	217.4	413.6
GLARE 3 3/2-0.3	1.40	61.7	232.1	514.6	60.8	228.7	512.6
GLARE 3 4/3-0.3	1.95	60.9	228.7	518.9	60.3	225.4	515.7
GLARE 3 5/4-0.3	2.50	60.2	224.6	522.4	59.4	220.3	518.2
GLARE 3 6/5-0.3	3.05	59.5	221.5	525.2	58.8	218.6	520.5
GLARE 3 3/2-0.4	1.70	63.4	236.2	506.5	62.9	233.7	503.7
GLARE 3 4/3-0.4	2.35	62.7	232.6	509.7	62.1	229.6	506.9
GLARE 3 5/4-0.4	3.00	62.2	228.7	511.6	61.3	225.4	508.8
GLARE 3 6/5-0.4	3.65	61.4	223.4	513.9	60.6	220.1	511.6
GLARE 3 3/2-0.5	2.00	65.3	240.3	497.8	64.8	236.4	494.2
GLARE 3 4/3-0.5	2.75	63.5	236.8	502.1	63.1	232.9	499.1
GLARE 3 5/4-0.5	3.50	62.9	232.4	506.3	62.2	228.7	504.6
GLARE 3 6/5-0.5	4.25	62.3	227.9	508.6	61.8	223.4	506.8

Table 4. Experimental data for GLARE 3-3,2 [9]

Test Nº1		Test Nº2		Test Nº3	
stress (Pa)	strain (%)	stress (Pa)	strain (%)	stress (Pa)	strain (%)
0	0.000	0	0.000	0	0.000
2,688	0.004	3,735	0.007	5,765	0.021
12,345	0.036	10,374	0.029	23,625	0.091
30,950	0.103	20,333	0.078	42,253	0.194
53,583	0.203	33,611	0.138	60,662	0.338
79,231	0.361	52,730	0.231	73,100	0.491
96,790	0.549	70,127	0.349	92,236	0.850
114,845	0.887	86,697	0.520	109,880	1.397
133,090	1.259	97,946	0.691	129,067	2.079
155,586	1.910	108,656	0.945	148,367	2.934
172,071	2.506	127,740	1.469	170,538	3.972
197,530	3.471	151,235	2.259	195,889	5.588
221,247	4.511	175,158	3.360	224,746	7.258
250,000	5.876	182,994	3.621	257,462	9.579
268,862	6.938	200,837	4.511	290,401	12.292
286,423	7.868	217,778	5.448	316,927	14.638
304,540	8.970	235,404	6.574	344,612	16.950
323,213	10.081	257,462	7.756	360,000	19.158
340,277	11.263	276,598	9.272	364,459	20.088
360,000	12.292	298,439	10.660		
375,723	13.440	316,927	12.083		
389,468	14.562	344,612	14.033		
410,549	15.896	371,197	16.136		
432,184	17.531	394,105	18.207		
454,375	19.158	420,096	20.412		
444,444	19.643	444,445	22.829		
		466,944	25.180		
		487,411	27.921		

Table 5. Theoretical Engineering Constants of constituents [12]

Material	E_x (GPa)	E_y (GPa)	σ_y (MPa)	σ_{ux} (MPa)	σ_{uy} (MPa)	Failure Strain ϵ (%)
Aluminium	73.8	73.8	295	484	465	16
Magnesium	45	45	170	220	204	15
Titanium	115	115	870	923	912	10
Glass/epoxy	53.98	9.41	192	790	85	4
Kevlar/epoxy	85.3	5.5	136	434	42	2.5
Carbon/epoxy	232	8.61	264	1170	123	1

Table 6. Engineering Constants of the adhesive [13]

E (GPa)	G_{Ic} $(kJ \cdot m^{-3})$	G_{IIc} $(kJ \cdot m^{-3})$	σ_{Ic} (MPa)	σ_{IIc} (MPa)
28	2.0	4.0	50	50